PROCEEDINGS OF SCIENCE

The sign problem in the ε-regime of QCD

K. Splittorff*
The Niels Bohr Institute, Blegdamsvej 17, DK-2100, Copenhagen Ø, Denmark
E-mail: split@nbi.dk

QCD in the ε-regime at nonzero baryon chemical potential μ is reviewed. The focus is on aspects of the sign problem which are relevant for lattice QCD. It is discussed how spontaneous chiral symmetry breaking and the sign problem are related through the spectrum of the Dirac operator. The strength of the sign problem is linked to the quark mass and the chemical potential. Specific implications for lattice QCD are discussed.

XXIVth International Symposium on Lattice Field Theory
July 23-28, 2006
Tucson, Arizona, USA

*Speaker.

PoS(LAT2006)023

1. Introduction

A way to understand lattice QCD at nonzero chemical potential, and the physics behind it, is to analyze the statistical properties of the Dirac eigenvalues. Twenty years ago [1, 2] it was realized that this approach apparently leads to a contradiction: At zero temperature a small (in units of the nucleon mass) chemical potential is expected to have a small effect on the chiral condensate, Σ. On the contrary the scatter plots of the Dirac spectrum obtained in lattice simulations [1, 3] leads one to conclude that Σ will vanish in the chiral limit for *any* nonzero value of the chemical potential. This conclusion was reached by means of an electrostatic analogy [1] where the chiral condensate is regarded as the electric field created by charges located at the position of the eigenvalues in the complex plane. The quark mass serves as a test charge inserted at the point $(m,0)$ in the complex plane where the electric field is measured. At zero chemical potential this analogy correctly leads to the Banks-Casher relation [4]. For a nonzero chemical potential the Dirac operator loses it anti-hermeticity and, consequently, the eigenvalues spread out into the complex eigenvalue plane. In the chiral limit the test charge (quark mass) moves to the center of this charge distribution and the chiral condensate hence vanishes for any nonzero chemical potential. The only way out seemed to be that a finite fraction of the eigenvalues would remain in a singular distribution (delta-function) on the imaginary axis at nonzero chemical potential. However, in unquenched QCD the sign problem creates a loophole in the electrostatic analogy. The unquenched spectral density of the QCD Dirac operator (the charge distribution) is a complex function which for for $\mu > m_\pi/2$ depends strongly on the quark mass (the test charge). Analytic calculations in the ε-regime [5] show that the complex valued spectral density has oscillations with a period inversely proportional to the volume and an amplitude that grows exponentially with the volume [6]. These oscillations lead to the discontinuity of the chiral condensate at zero quark mass [7]. Spontaneous chiral symmetry breaking is therefore intimately related to the sign problem. Because the oscillations of the eigenvalue density take place on a scale inversely proportional to the volume, the microscopic scaling of the ε-regime is required to resolve the individual oscillations and hence the way in which the discontinuity of the chiral condensate is built up form the eigenvalue density.

In quenched QCD there is of course no sign problem and the electrostatic analogy is in fact valid. By solving a random matrix model for QCD at the mean field level it was argued in [8] that quenched QCD at nonzero chemical potential is the zero flavor limit of QCD with nonzero isospin chemical potential. Indeed, the chiral condensate vanishes in the chiral limit for any nonzero isospin chemical potential [9, 10, 11]. Lattice simulations [12, 13, 14] have already been successfully compared to the quenched microscopic eigenvalue density computed in [15].

The complex oscillations of the unquenched eigenvalue density is a manifestation of the sign problem. The oscillations appear for $\mu > m_\pi/2$. In the ε-regime it is also possible to compute the unquenched average of the phase factor of the fermion determinants and thereby to measure the strength of the sign problem directly [16]. It is shown that the average phase factor goes to zero at $\mu = m_\pi/2$ and remains at zero for $\mu > m_\pi/2$. The sign problem is therefore particularly acute for $\mu > m_\pi/2$. It is not surprising that the sign problem sets in at $\mu = m_\pi/2$. Suppose we had neglected the sign problem, that is, replaced the fermion determinant in the partition function by its absolute value. Since conjugating a fermion determinant corresponds to changing the sign of the chemical potential [17] the free energy would have a second order discontinuity at $\mu = m_\pi/2$

signaling the formation of a Bose condensate of pions [9]. Reinserting the phase factor of the fermion determinant must wipe out this Bose condensate completely and hence the complex nature of the fermion determinant must be particularly important for $\mu > m_\pi/2$. Since we know the physical origin of the scale $\mu = m_\pi/2$ we can understand the behavior of the sign problem at nonzero temperature and chemical potential. This allows us to make contact to lattice simulations [18, 19, 20, 21, 22] at nonzero temperature and chemical potential.

This review is organized as follows. We first define the ε-regime and briefly discuss two independent ways to compute the microscopic spectral correlation functions. Then we analyze the unquenched eigenvalue density in detail. In section 4 we show how the oscillations of the eigenvalue density lead to the discontinuity of the chiral condensate. Finally we discuss the strength of the sign problem and the consequences for lattice simulations.

2. The ε-regime at nonzero chemical potential

In order to extend the Banks-Casher relation to nonzero chemical potential it would be helpful to know the eigenvalue density of the Dirac operator near the origin, in the phase where chiral symmetry is spontaneously broken, for small μ and m. Remarkably, in the ε-regime it is possible to get all this. By definition [23] the ε-regime deals with the phase where chiral symmetry is spontaneously broken. The quark mass and chemical potential are taken such that (V is the 4-volume and F_π is the pion decay constant)

$$m\Sigma \sim \frac{1}{V} \quad \text{and} \quad \mu^2 F_\pi^2 \sim \frac{1}{V}. \tag{2.1}$$

The correlations of the Dirac eigenvalues, z, are considered on the microscopic scale [24] where

$$z\Sigma \sim \frac{1}{V}. \tag{2.2}$$

The original work on the ε-regime [23] focused on the quark mass dependence of the finite volume partition function and shows how the chiral condensate goes to zero if the quark mass is taken to zero in a finite but large volume. The effect of the chemical potential on the finite volume partition function is determined by the flavor symmetries and the scaling of the chemical potential with the volume. Using the GOR relation and (2.1) it follows that the chemical potential, in the ε-regime, is of the same order as the pion mass. With this scaling the Compton wavelength of the pion is much larger than the linear size of the volume and the effective partition function reduces to a group integral over the static modes of the pion field uniquely determined by the pattern of chiral symmetry breaking [25]

$$Z_{N_f}(\{m_f\};\mu) = \int_{U\in U(N_f)} dU \ \det(U)^\nu \ \mathrm{e}^{-\frac{V}{4}F_\pi^2\mu^2 \mathrm{Tr}[U,B][U^{-1},B] \ + \ \frac{1}{2}\Sigma V \mathrm{Tr} M(U+U^{-1})}. \tag{2.3}$$

Both M and B are diagonal matrices. M is the quark mass matrix and B contains the quark baryon charges. Since here all quarks have the same baryon charge the B matrix is proportional to the unit matrix and the dependence on the chemical potential automatically drops out of the partition function (2.3). This is exactly as expected, since the pions have baryon charge zero, the chemical potential is inert.

2.1 The eigenvalue density

The zero temperature effective partition function does not depend on the chemical potential even though the eigenvalues of the Dirac operator do[1]. The chemical potential adds a hermitian part to the Dirac operator and the eigenvalue spectrum,

$$(D+\mu\gamma_0)\psi_j = z_j\psi_j, \tag{2.4}$$

is no longer purely imaginary. The support of the eigenvalue density

$$\rho_{N_f}(z,z^*,\{m_f\};\mu) \equiv \left\langle \sum_j \delta^2(z-z_j) \right\rangle_{N_f}, \tag{2.5}$$

is therefore two dimensional domain in the complex eigenvalue plane. Here we have used the notation

$$\langle \mathscr{O} \rangle_{N_f} \equiv \frac{\int dA\ \mathscr{O}\ \prod_{f=1}^{N_f} \det(D+\mu\gamma_0+m_f)\ e^{-S_{YM}}}{\int dA \prod_{f=1}^{N_f} \det(D+\mu\gamma_0+m_f)\ e^{-S_{YM}}}. \tag{2.6}$$

The eigenvalue density is the function which allows us to turn the average of a sum over eigenvalues, e.g. $\langle \sum 1/(z_j+m)\rangle$, into an integral, $\int d^2z\ \rho/(z_j+m)$. However, due to the presence of the complex fermion determinant in the measure (the sign problem) the unquenched eigenvalue density is not expected to be real and positive.

The eigenvalue density in the ε-regime, also known as the microscopic eigenvalue density, describes the eigenvalues in a range of order $1/\Sigma V$ from the origin. At present there exist two independent ways to compute the microscopic correlation functions of the QCD Dirac operator at nonzero baryon chemical potential. One can obtain them directly from the effective partition functions [15, 6] writing the δ-functions in (2.5) by means of the replica trick [8, 27]

$$\rho_{N_f}(z,z^*,\{m_f\};\mu) = \frac{1}{Z_{N_f}} \lim_{n\to 0} \frac{1}{n} \partial_z \partial_{z^*} \int dA |\det(D+\mu\gamma_0+z)|^{2n} \prod_{f=1}^{N_f} \det(D+\mu\gamma_0+m_f)\ e^{-S_{YM}}. \tag{2.7}$$

Note that the integral is a partition function with n additional quarks and conjugate quarks. The conjugate quarks corresponds to quarks with the opposite baryon charge [17] and this is why these partition functions and hence the eigenvalue density depend on μ. We refer to these partition functions as the generating functionals for the eigenvalue density.

Alternatively one can start from a chiral random matrix theory and use biorthogonal polynomials in the complex plane [28, 29, 30, 5]. For an up-to-date review of the random matrix approach to QCD at nonzero chemical potential, see [31]. (In principle, one can also make use of the supersymmetric method [32].)

The microscopic eigenvalue density of the Dirac operator in quenched QCD was first obtained from effective partition functions like (2.3) in [15] and subsequently reproduced from the random matrix methods [5]. The expression for the quenched eigenvalue density is

$$\rho_{N_f=0}(z,z^*;\mu) = \frac{|z|^2\Sigma^4V^3}{2\pi\mu^2F_\pi^2} e^{-2\mu^2F_\pi^2V} e^{-\frac{(z^2+z^{*2})\Sigma^2V}{8\mu^2F_\pi^2}} K_0\left(\frac{|z|^2\Sigma^2V}{4\mu^2F_\pi^2}\right) \int_0^1 dt\, t e^{-2\mu^2F_\pi^2Vt^2} I_0(z\Sigma V) I_0(z^*\Sigma V). \tag{2.8}$$

[1] To understand how this is possible is frequently referred to as *the silver blaze problem* [26].

The unquenched eigenvalue density, on the other hand, was derived first by means of the random matrix techniques [5] and subsequently derived using the replica trick [6]. Here we give the result for one flavor in the topologically trivial sector (see [5, 6] for the general expressions)

$$\rho_{N_f=1}(z,z^*,m;\mu) \;=\; \rho_{N_f=0}(z,z^*;\mu)\left(1-\frac{I_0(z\Sigma V)\int_0^1 dt te^{-2\mu^2F_\pi^2Vt^2}I_0(m\Sigma V)I_0(z^*\Sigma V)}{I_0(m\Sigma V)\int_0^1 dt te^{-2\mu^2F_\pi^2Vt^2}I_0(z\Sigma V)I_0(z^*\Sigma V)}\right). \quad (2.9)$$

Note that the unquenched density is the sum of the quenched density and a term from unquenching $\rho_{N_f=1}(z,z^*,m;\mu)=\rho_{N_f=0}(z,z^*;\mu)+\rho_U(z,z^*,m;\mu)$ and that the density is zero for $m=z$.

3. A complex and oscillating eigenvalue density

The eigenvalue z and its complex conjugate z^* do not enter symmetrically in the unquenching part of the eigenvalue density (2.9). This suggests that the unquenched eigenvalue density is in general a complex function. Here we take a closer look at the unquenched eigenvalue density of the QCD Dirac operator and identify the scale at which it becomes complex.

For infinitely large quark mass the unquenching term in (2.9) is suppressed and the eigenvalue density is constant and nonzero in a strip along the imaginary axis of width $2\mu^2F_\pi^2/\Sigma$. The quark mass enters the strip of eigenvalues when $m<2\mu^2F_\pi^2/\Sigma$ or, equivalently, when $m_\pi<2\mu$. After the quark mass has entered this strip the unquenched eigenvalue density is dramatically different from the quenched eigenvalue density. Starting at $z=\pm m$ and extending to the support of the eigenvalue density are two regions in which the unquenched eigenvalue density is complex and oscillating. Figures 1 and 2 illustrate the appearance of the oscillating regions for $2\mu>m_\pi$. The oscillations have an amplitude which grows exponentially with the volume and have a period inversely proportional to the volume. This structure has a physical origin: The generating functionals for the eigenvalue density in (2.7) are partition functions with additional pairs of conjugate fermions (for explicit evaluation of these partition functions in the ε-regime see [15, 33]). The three regions of the unquenched eigenvalue density correspond to three phases of the generating functionals [7, 34, 35]. The uniform part of the density corresponds to the phase with a condensate of pions made op of the quarks with masses z and z^*. This pion condensate forms when 2μ exceeds the mass of these pions, $(2\mu)^2>2Re[z]\Sigma/F_\pi^2$. This why the with of the strip of eigenvalues is $Re[z]<2\mu^2F_\pi^2/\Sigma$. The oscillating region corresponds to a phase with Bose condensation of pions of squared mass $(m+z^*)\Sigma/F_\pi^2$. This condensate dominates for $m<z$ since in this case the squared mass, $(m+z^*)\Sigma/F_\pi^2$, of these pions is smaller than the squared mass, $(z+z^*)\Sigma/F_\pi^2$, of the pions made up of the quarks with masses z and z^*. Finally, the region outside the support of the eigenvalue density corresponds to the normal phase, without Bose condensates, of the generating functionals.

To see how the structure emerges from (2.9) let us look at the limit where the width of the eigenvalue support is large, $2\mu^2F_\pi^2V\gg1$, and where the quark mass and eigenvalue is inside the support and well away from the origin ($m\Sigma V\gg1$, $|z|\Sigma V\gg1$). In this case the unquenched eigenvalue density simplifies to ($z=x+iy$)

$$\rho_{N_f=1}(x,y,m;\mu)\sim\frac{1}{4\mu^2F^2V}(1-e^{V\Sigma\left[\frac{\Sigma(x^2-y^2+m^2)}{8\mu^2F_\pi^2}-\frac{\Sigma x^2}{2\mu^2F_\pi^2}+\frac{\Sigma xm}{4\mu^2F_\pi^2}+x-m\right]}e^{iV\Sigma y\left(1-\frac{\Sigma(x+m)}{4\mu^2F_\pi^2}\right)}). \quad (3.1)$$

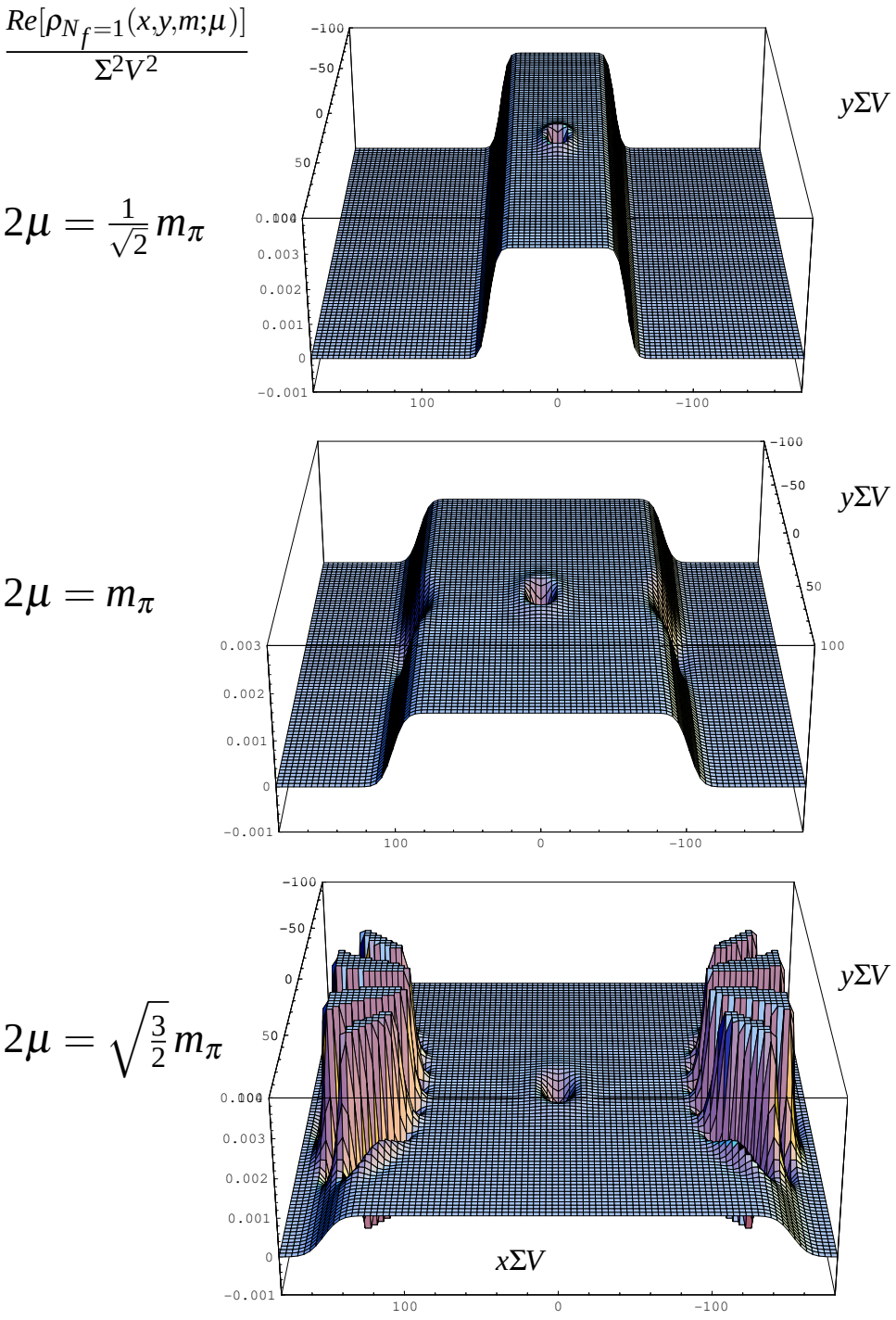

Figure 1: The real part of the microscopic eigenvalue density of the QCD Dirac operator for fixed quark mass $m\Sigma V = 100$. The chemical potential increases from the top and down such that the width $2\mu^2 F_\pi^2 V = 50$, 100, 150. To the left of the plots the chemical potential is expressed in terms of the pion mass. Note that the support of the eigenvalue distribution reaches the quark mass when $\mu = m_\pi/2$. As μ exceeds this value two oscillating regions starts at $z = \pm m$ and extend towards the edge of the support.

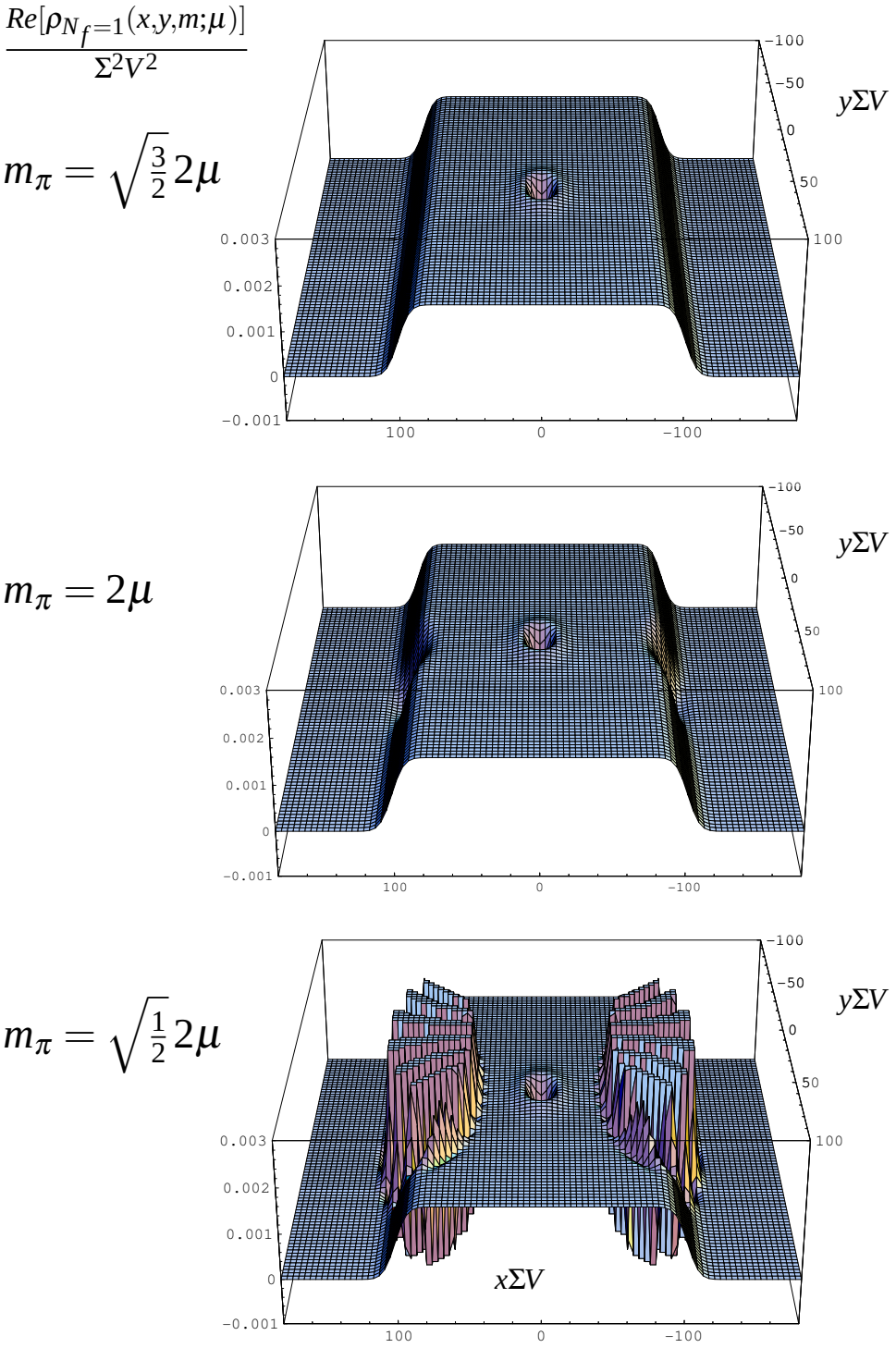

Figure 2: The unquenched eigenvalue density for fixed chemical potential $2\mu^2F_\pi^2V = 100$ and decreasing quark mass $m\Sigma V = 150, 100, 50$. The pion mass in units of the chemical potential is given to the left of the plots. Inside the oscillating regions the imaginary part of the eigenvalue density is nonzero and oscillates out of phase with the real part shown. Note that the oscillations by far exceeds the scale of the plot.

The term independent of x and y (the $'1'$) gives the plateau of the quenched part (since we assumed that the eigenvalue was inside the strip we do not see the boundary at $x = 2\mu^2 F_\pi^2/\Sigma$). The second term gives the effect of unquenching, it is exponentially suppressed or enhanced with the volume depending on the sign in the square bracket. This gives the boundary of the oscillating region. Finally, from the oscillating exponential it is clear that the period of the oscillations is of order $1/V$. For x and m well inside the support the oscillations are predominantly along the imaginary axis.

The oscillations are of course a manifestation of the sign problem so we should expect that the sign problem is acute for $\mu > m_\pi/2$. We will confirm this expectation in section 6.

4. The Banks-Casher relation at nonzero μ

At zero chemical potential the accumulation of eigenvalues at the origin on the imaginary axis is responsible for chiral symmetry breaking [4]. As we discuss now the oscillations of the eigenvalue density are responsible for chiral symmetry breaking at $\mu \neq 0$ [7].

Using the definition of the eigenvalue density (2.5) the chiral condensate can be expressed as an integral over the complex eigenvalue plane

$$\Sigma_{N_f}(m;\mu) = \int d^2z \, \frac{\rho_{N_f}(z,z^*,m;\mu)}{z+m}. \tag{4.1}$$

As noted below eq. (2.9) is it natural to write the unquenched eigenvalue density as a sum of two terms

$$\rho_{N_f}(z,z^*,m;\mu) = \rho_{N_f=0}(z,z^*;\mu) + \rho_U(z,z^*,m;\mu), \tag{4.2}$$

where $\rho_U(z,z^*,m;\mu)$ is what is left after subtracting the quenched density. See the left hand column of figure 3. The quenched density is by definition real and positive so, in agreement with our asymptotic analysis above, the complex oscillations reside entirely in $\rho_U(z,z^*,m;\mu)$. Inserting $\rho_{N_f} = \rho_{N_f=0} + \rho_U$ in (4.1) shows that the chiral condensate is built up from two terms

$$\Sigma_{N_f} = \Sigma_Q + \Sigma_U. \tag{4.3}$$

The individual contributions to the chiral condensate are shown the right hand column of figure 3. As expected from lattice simulations and the electrostatic analogy the quenched contribution drops to zero in the chiral limit. The entire discontinuity of the chiral condensate thus comes from the oscillating part, cf. the lower row of figure 3. To see analytically how the oscillations of the eigenvalue density build up the discontinuity, insert the asymptotic form (3.1) in (4.1) and first perform the integral over y for fixed x by going to the complex $y = a + ib$ plane [7]. In this plane the roles of the two exponentials in (3.1) are mixed: Since there is an explicit factor of V in both arguments, the second exponential now also affects the boundary of the oscillating region (this is why it is essential that the oscillations have a period of order $1/V$ and an amplitude which is exponentially large in the volume). Due to the mixing the contour can be deformed into a region where the integrand is exponentially suppressed. The y-integral through the oscillating part is therefore given by the residue at the pole alone. The residue follows automatically from the observation that the unquenched eigenvalue density vanishes at $z = m$ [7].

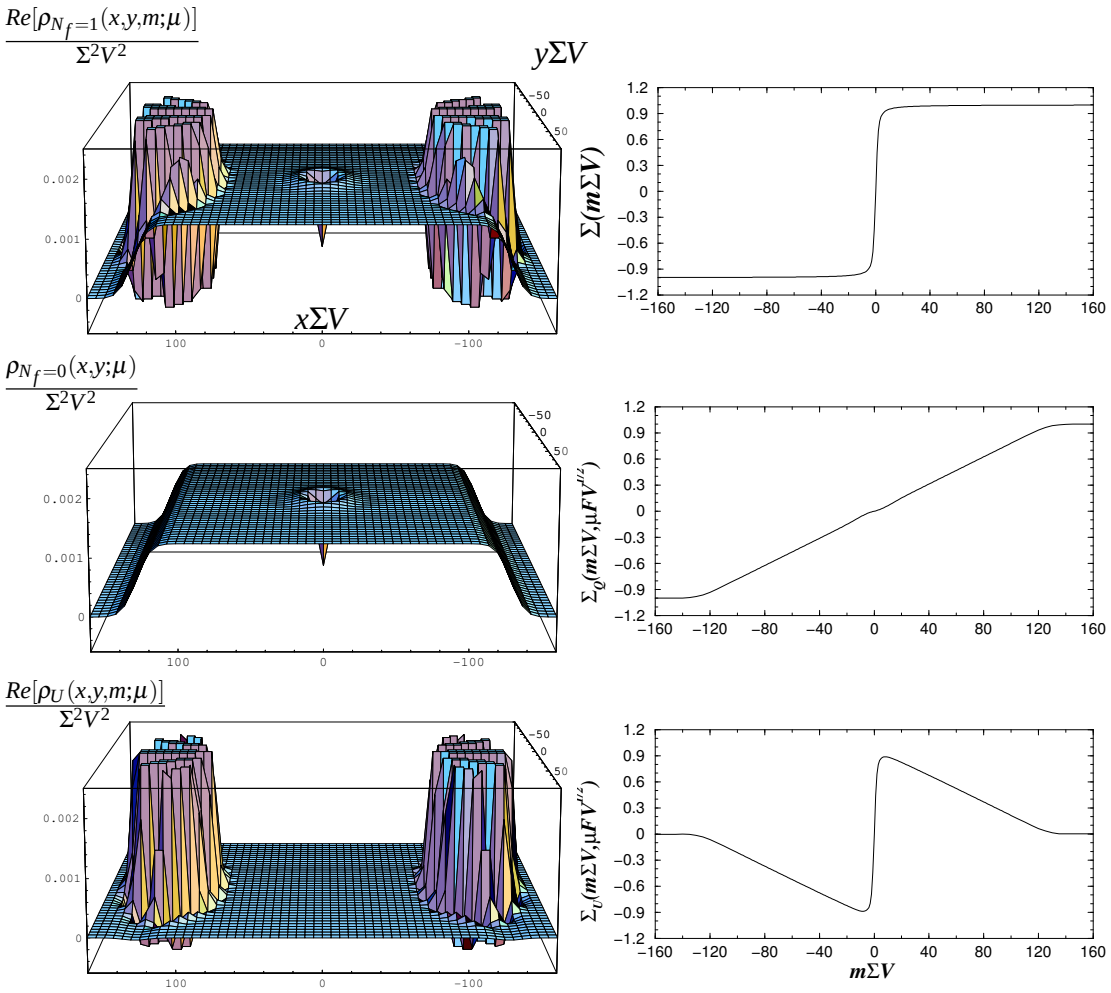

Figure 3: Left column: The unquenched eigenvalue density (top) split into the quenched part (middle) and the oscillating part (bottom). **Right column:** The chiral condensate as a function of the quark mass. The top panel shows the full chiral condensate and the two plots below give the individual contributions from the quenched eigenvalue density and the oscillating region respectively. Note that it is the oscillations of the eigenvalue density which are responsible for the discontinuity of the chiral condensate at zero quark mass.

5. Lattice simulations in the ε-regime at $\mu \neq 0$

The sign problem in QCD occurs since the baryon chemical potential introduces a mismatch between quarks and anti-quarks. If we instead consider a chemical potential for the third component of isospin then the anti-particle is a part of the measure which therefore remains real [17]. Quenched QCD with $\mu \neq 0$ is the zero flavor limit of QCD at nonzero isospin chemical potential [8]. The microscopic eigenvalue density (2.8) in the quenched case has been compared successfully to staggered lattice simulations [12, 13] as well as to simulations of a Ginsparg-Wilson Dirac operator at nonzero chemical potential [14]. The measure of 2 color QCD at nonzero baryon chemical potential is also real and this has allowed to test the predictions for the microscopic spectral density [38] in the quenched case [39] as well as the unquenched [40].

If the baryon chemical potential is purely imaginary the Dirac operator remains anti-hermitian. The correlations between two such Dirac operators separated by a microscopic difference between the values of the imaginary chemical potential is extremely sensitive to the value of F_π. The correlation function thus provides a way to extract the pion decay constant from simulations in the ε-regime [41].

6. The strength of the sign problem

The analysis of the spectra of the QCD Dirac operator has shown that the sign problem manifest itself in the eigenvalue density when $\mu > m_\pi/2$. This is precisely the value of μ for which the eigenvalue density reaches the quark mass and thus where eigenvalues, z, for which $(z-m) \sim 1/\Sigma V$ become frequent. In order to quantify the strength of the sign problem let us write

$$\det(D+\mu\gamma_0+m) = |\det(D+\mu\gamma_0+m)|e^{i\theta} \tag{6.1}$$

and consider the expectation value of the (squared) phase factor of the fermion determinant

$$\left\langle e^{2i\theta}\right\rangle_{N_f} = \left\langle \frac{\det(D+\mu\gamma_0+m)}{\det(D+\mu\gamma_0+m)^*}\right\rangle_{N_f} = \frac{Z_{N_f+1|1^*}}{Z_{N_f}}. \tag{6.2}$$

For $\mu = 0$ the phase, θ, is zero and $\langle e^{2i\theta}\rangle = 1$. If the fluctuations drives $\langle e^{2i\theta}\rangle$ to zero the sign problem is very strong.

The expectation value of the phase factor is equal to the partition function ($Z_{N_f+1|1^*}$) with an additional fermionic flavor and an additional conjugate bosonic flavor divided by the standard dynamical partition function (Z_{N_f}). In the ε-regime these partition functions can be evaluated explicitly [42, 16]. The thermodynamic limit, $m\Sigma V \to \infty$ and $\mu^2 F_\pi^2 V \to \infty$, of the result is extremely simple. The sign problem has two distinct phases (see figure 4): For $\mu < m_\pi/2$ the sign problem saturates at a nonzero value

$$\left\langle e^{2i\theta}\right\rangle_{N_f} = (1-\frac{4\mu^2}{m_\pi^2})^{N_f+1} e^{V0} \quad \text{for} \quad \mu < m_\pi/2. \tag{6.3}$$

In the other phase the sign problem is exponentially bad in the volume

$$\left\langle e^{2i\theta}\right\rangle_{N_f} \sim e^{-VF_\pi^2 \frac{(m_\pi^2-4\mu^2)^2}{8\mu^2}} \quad \text{for} \quad \mu > m_\pi/2. \tag{6.4}$$

The behavior of the phase follows directly from leading order chiral perturbation theory [16]. At leading order the low energy effective partition function is given by a saddle point approximation

$$Z^{\rm LO} \sim J\sqrt{\frac{\prod_f Vm_{\pi,f}^2}{\prod_b Vm_{\pi,b}^2}} e^{-V\Omega_{MF}}, \tag{6.5}$$

where $m_{\pi,b}$ ($m_{\pi,f}$) are the masses of the Goldstone bosons (fermions). (The Goldstone fermions are made up of a fermionic quark and a bosonic conjugate quark.) The free energy density Ω_{MF} is given by the Lagrangian at the mean field value of the fields. Finally, J is the Jacobian from the measure.

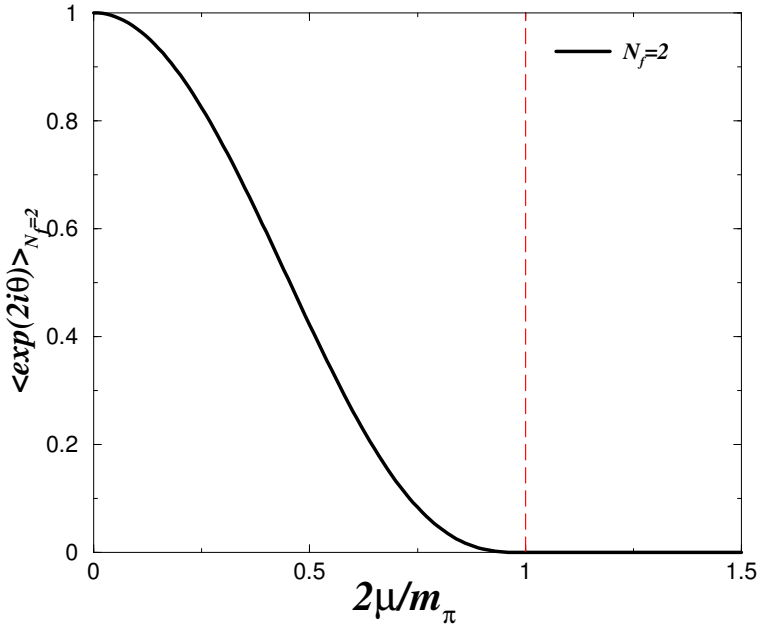

Figure 4: The expectation value of the phase factor of the fermion determinant in QCD with two dynamical flavors. Shown is the curve for $\mu F_\pi \sqrt{V} \gg 1$. In this limit of the ε-regime $\langle \exp(2i\theta)\rangle$ only depends on the ratio $2\mu/m_\pi$.

For $\mu < m_\pi/2$ the additional fermionic and bosonic quark in the numerator of (6.2) has no effect on the mean field free energy. The factors of $\exp(-V\Omega_{\rm MF})$ hence cancel between the numerator and denominator in (6.2). For $\mu > m_\pi/2$ the partition function in the numerator is in a Bose condensed phase and, consequently, the mean field free energy in the numerator does not match that in the denominator. This leads to an expectation value of the phase which is exponentially small in the volume.

The saddle point approximation, (6.5), also allow us to understand the preexponential factor in (6.3). The masses of the charged pions do depend on μ even for $\mu < m_\pi/2$ [43, 44, 9]. The charged pions are the ones made up from a fermionic quark and a bosonic conjugate quark. There are $2(N_f+1)$ such Goldstone fermions, half of which have mass $m_\pi - 2\mu$ while the other half have mass $m_\pi + 2\mu$. The resulting overall factor $(m_\pi^2 - 4\mu^2)^{N_f+1}$ is divided by $m_\pi^{2(N_f+1)}$ which is left after canceling out the neutral Goldstone bosons from the partition function in the denominator. This explains the result (6.3) for $\langle e^{2i\theta}\rangle_{N_f}$ when $\mu < m_\pi/2$.

Since $\langle e^{2i\theta}\rangle_{N_f}$ is a ratio of two partition functions it is real. The same is true for $\langle e^{-2i\theta}\rangle_{N_f}$ implying that $\langle \sin(2\theta)\rangle_{N_f}$ is purely imaginary. To see that $\langle \sin(2\theta)\rangle_{N_f}$ is nonzero we need to compute $\langle e^{-2i\theta}\rangle_{N_f}$ and show that it is different from $\langle e^{2i\theta}\rangle_{N_f}$. The expectation value of the inverse phase factor also has a very simple form in the thermodynamic limit

$$\left\langle e^{-2i\theta}\right\rangle_{N_f} = (1-\frac{4\mu^2}{m_\pi^2})^{-N_f+1} e^{V0} \quad \text{for} \quad \mu < m_\pi/2. \tag{6.6}$$

The expectation value of the inverse phase is *not* equal to the expectation of the phase. They are

only equal in quenched and phase quenched QCD where the weight function is real.

Note that lattice tests of the predictions for $\langle e^{2i\theta}\rangle$ are possible for $\mu < m_\pi/2$ even in unquenched QCD. Related observables has been measured on the lattice [36, 37, 19].

7. Nonzero temperature

Unquenched lattice simulations at nonzero chemical potential must deal with the sign problem. At present three major approaches have been explored, the multi parameter reweighting method [18], the Taylor expansion method [19, 20], and analytic continuation from imaginary chemical potential [21, 22]. See also the plenary review at this lattice conference by C. Schmidt [45].

Above we computed the strength of the sign problem and found that it changes drastically when $\mu = m_\pi/2$. The fact that the change takes place at $\mu = m_\pi/2$ has a physical origin: $\langle \exp(2i\theta)\rangle$ is a ratio of two partition functions, c.f. (6.2), and since the partition function in the numerator includes a conjugate quark it experiences a phase transition into a Bose condensed phase at this value of μ. The Bose condensate changes the functional form of the free energy and causes an exponential suppression of $\langle \exp(2i\theta)\rangle$ for $\mu > m_\pi/2$. The region in the μ, T-plane for which this Bose condensate is present is therefore identical to the region where $\langle \exp(2i\theta)\rangle$ is exponentially suppressed. As we have argued above the chemical potential above which the quark mass is inside the support of the eigenvalue density is also determined by Bose condensation of weakly interacting pions. The region of the μ, T-plane where the sign problem is exponentially suppressed is therefore identical to the region where the quark mass is inside the support of the eigenvalue density. This region is below the thick line indicated in figure 5. As the temperature is increased the line bends to the right since for a sufficiently high temperature the Bose condensate will melt. The curve gives the melting temperature of the Bose condensate as calculated in [10]. It is consistent with the melting temperature computed in phase quenched lattice QCD [11].

The lattice computations of [19] suggests that the strength of the sign problem scales with the critical chemical potential: In the left panel of figure 5 we show contour lines from [19] of the variance of the two flavor staggered fermion determinant, in our notation $\sqrt{\langle (2\theta)^2\rangle - \langle 2\theta\rangle^2}$. The lines give the contours up to the value 2π in steps of $\pi/4$. The contours are parallel to the thick line indicating the expected critical chemical potential for which the quark mass hits the support of the eigenvalue density and the sign problem becomes very severe [46].

Almost all of the lattice simulations [18, 19, 20, 21, 22] address the region of the μ, T-plane where the sign problem is less severe. One exception is [18]. These two studies of the critical endpoint used two sets of quark masses. The endpoint was found to depend strongly on the quark mass. In fact, as observed in [20], the value of the chemical potential at the endpoint scales like pion mass in these studies. In the right hand part of figure 5 we give the location of the endpoints found in [18] together with the line where the quark mass is expected to hit the support of the eigenvalue density. Surprisingly both endpoints points are located very close to the line [46]. To the right of the line the sign problem is exponentially strong and this has been argued [37] to invalidate the Yang-Lee analysis used in [18]. Moreover, when the quark mass is inside the support of the eigenvalue density the 4th root trick used in [18] may be illdefined [47]. For these reasons one may fear that the signals interpreted as a signature of the endpoint in [18] is rather a breakdown of the method used.

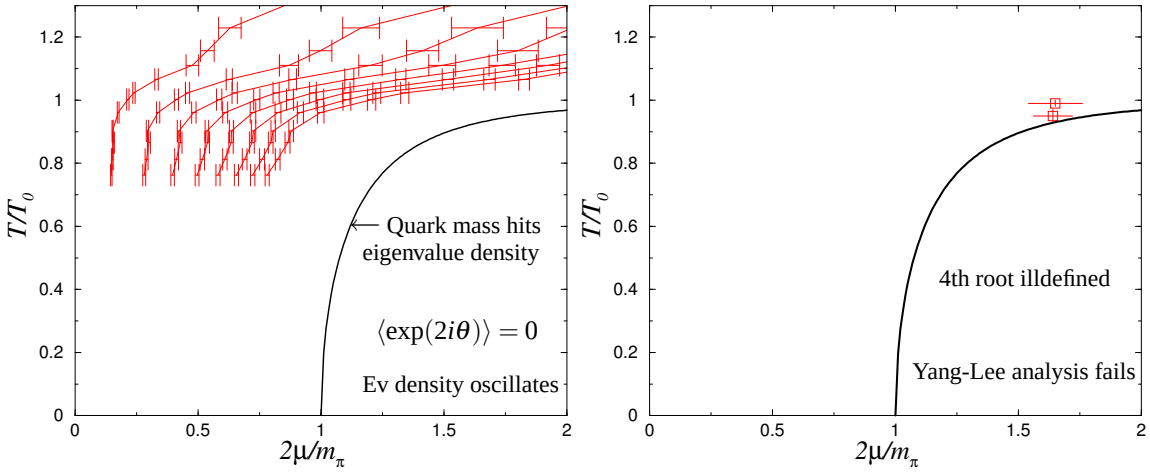

Figure 5: Left: Contour lines of the variance $\sqrt{\langle\theta^2\rangle-\langle\theta\rangle^2}=\pi/4,2\pi/4,\ldots 2\pi$ of the phase of the fermion determinant from [19]. Note that the variance depends on the distance from the line where the quark mass hits the support of the eigenvalue spectrum (indicated by the thick line). **Right:** The measured endpoints from [18] and the line where the quark mass hits the eigenvalue density. To the right of this line the Yang-Lee analysis [37] and the 4th root trick [47] used in [18] are troublesome.

8. Summary

The study of the ε-regime of QCD at nonzero chemical potential has provided new insights in QCD which go beyond the microscopic scale. Here we have reviewed those aspects which have direct relevance for the sign problem in lattice QCD. The non-hermitian nature of the Dirac operator at $\mu\neq 0$ also have a very nontrivial effect on the analytical methods which where used to derive the results discussed here. For a review focused on these aspects, see [31].

Here we have discussed how the analysis of the spectrum of the QCD Dirac operator allows us to understand the sign problem in lattice QCD at nonzero chemical potential. From the perspective of the Dirac operator the sign problem plays an all important role for spontaneous chiral symmetry breaking. The sign problem induces violent complex oscillations in the spectral density of the Dirac operator and these in turn build up the entire discontinuity of the chiral condensate in the chiral limit. Therefore, to address spontaneous chiral symmetry breaking in the chiral limit on the lattice at $\mu\neq 0$, one must deal with the sign problem.

The strength of the sign problem can be measured by the average of the phase factor, $\langle\exp(2i\theta)\rangle$. In general $\langle\exp(2i\theta)\rangle$ depends on quark mass, the chemical potential, the volume, the temperature as well as the lattice cutoff. In the ε-regime we can quantify the dependence of $\langle\exp(2i\theta)\rangle$ on μ and the quark mass: $\langle\exp(2i\theta)\rangle$ is nonzero for $\mu<m_\pi/2$ while for $\mu>m_\pi/2$ it is exponentially small in the volume. The separation between these two scales is linked to the onset of Bose condensation and this physical insight allows us to extrapolate the results beyond the ε-regime. For $\mu>m_\pi/2$ we expect that there is a critical temperature at which the sign problem changes its nature. Care should be taken not to misinterpret manifestations of this change in lattice QCD.

Acknowledgments: It is a privilege to thank Jac Verbaarschot, Gernot Akemann, James Osborn, Dominique Toublan, Poul Henrik Damgaard, Urs Heller and Benjamin Svetitsky for collaborations. My warmest tanks also to the organizers of lattice 2006 for creating a perfect work environment. The author is supported by the Carlsberg Foundation.

References

[1] I. Barbour, N-E. Behilil, E. Dagotto, F. Karsch, A. Moreo, M. Stone and H. W. Wyld, Nucl. Phys. B **275** (1986) 296.

[2] Philip E. Gibbs, Phys. Lett. B **182** (1986) 369.

[3] J. B. Kogut, H. Matsuoka, M. Stone, H. W. Wyld, S. H. Shenker, J. Shigemitsu and D. K. Sinclair, Nucl. Phys. B **225**, 93 (1983); M. P. Lombardo, J. B. Kogut and D. K. Sinclair, Phys. Rev. D **54** (1996) 2303; S. Hands, I. Montvay, L. Scorzato and J. Skullerud, Eur. Phys. J. C **22**, 451 (2001).

[4] T. Banks and A. Casher, Nucl. Phys. **B169**, 103 (1980).

[5] J. C. Osborn, Phys. Rev. Lett. **93**, 222001 (2004).

[6] G. Akemann, J. C. Osborn, K. Splittorff and J. J. M. Verbaarschot, Nucl. Phys. B **712**, 287 (2005).

[7] J. C. Osborn, K. Splittorff and J. J. M. Verbaarschot, Phys. Rev. Lett. **94**, 202001 (2005).

[8] M. Stephanov, Phys. Rev. Lett. **76**, 4472 (1996).

[9] D. T. Son and M. A. Stephanov, Phys. Rev. Lett. **86**, 592 (2001); K. Splittorff, D. Toublan, and J.J.M. Verbaarschot, Nucl. Phys. B **620**, 290 (2002); Nucl. Phys. B **639**, 524 (2002).

[10] B. Klein, D. Toublan and J. J. M. Verbaarschot, Phys. Rev. D **68** (2003) 014009.

[11] J.B. Kogut and D.K. Sinclair, Phys. Rev. D **66**, 034505 (2002).

[12] G. Akemann and T. Wettig, Phys. Rev. Lett. **92**, 102002 (2004) [Erratum-ibid. **96**, 029902 (2006)].

[13] J. C. Osborn and T. Wettig, PoS **LAT2005**, 200 (2006).

[14] J. Bloch and T. Wettig, Phys. Rev. Lett. **97**, 012003 (2006).

[15] K. Splittorff and J. J. M. Verbaarschot, Nucl. Phys. B **683**, 467 (2004).

[16] K. Splittorff and J. J. M. Verbaarschot, hep-lat/0609076.

[17] M. Alford, A. Kapustin, and F. Wilczek, Phys. Rev. **D 59** (1999) 054502.

[18] Z. Fodor and S. D. Katz, JHEP **0404**, 050 (2004); JHEP **0203**, 014 (2002).

[19] C. R. Allton *et al.*, Phys. Rev. D **71**, 054508 (2005); C. R. Allton, S. Ejiri, S. J. Hands, O. Kaczmarek, F. Karsch, E. Laermann and C. Schmidt, Phys. Rev. D **68**, 014507 (2003); C. R. Allton *et al.*, Phys. Rev. D **66**, 074507 (2002).

[20] R. V. Gavai and S. Gupta, Phys. Rev. D **68**, 034506 (2003); Phys. Rev. D **71**, 114014 (2005).

[21] P. de Forcrand and O. Philipsen, hep-lat/0607017; Nucl. Phys. B **673**, 170 (2003); Nucl. Phys. B **642**, 290 (2002).

[22] M. D'Elia and M. P. Lombardo, Phys. Rev. D **67**, 014505 (2003).

[23] J. Gasser and H. Leutwyler, Phys. Lett. B **188**, 477 (1987), H. Leutwyler and A. Smilga, Phys. Rev. D **46**, 5607 (1992).

[24] E.V. Shuryak and J.J.M. Verbaarschot, Nucl. Phys. A 560 (1993) 306; J.J.M. Verbaarschot, Phys. Rev. Lett. 72 (1994) 2531; Phys. Lett. B 368 (1996) 137.

[25] D. Toublan and J. J. M. Verbaarschot, Int. J. Mod. Phys. B **15**, 1404 (2001).

[26] T. D. Cohen, Phys. Rev. Lett. **91**, 222001 (2003).

[27] K. Splittorff and J.J.M. Verbaarschot, Phys. Rev. Lett. **90**, 041601 (2003).

[28] G. Akemann and G. Vernizzi, Nucl. Phys. B **660** (2003) 532.

[29] G. Akemann, Acta Phys. Polon. B **34** (2003) 4653.

[30] M.C. Bergère, hep-th/0311227; hep-th/0404126.

[31] G. Akemann, *in preparation.*

[32] K.B. Efetov, Phys. Rev. Lett. **79**, 491 (1997); Adv. Phys. **32**, 53 (1983), *Supersymmetry in disorder and chaos*, (Cambridge University Press, Cambridge, 1997); Y.V. Fyodorov, B.A. Khoruzhenko and H.-J. Sommers, Phys. Lett. A226 (1997) 46; Y.V. Fyodorov and H.-J. Sommers, J. Math. Phys. 38 (1997) 1918.

[33] G. Akemann, Y. V. Fyodorov and G. Vernizzi, Nucl. Phys. B **694**, 59 (2004).

[34] J. C. Osborn, K. Splittorff and J. J. M. Verbaarschot, Int. J. Mod. Phys. A **21**, 859 (2006).

[35] J. B. Kogut and D. Toublan, Phys. Rev. D **64**, 034007 (2001).

[36] Y. Sasai, A. Nakamura and T. Takaishi, Nucl. Phys. Proc. Suppl. **129**, 539 (2004).

[37] S. Ejiri, 'Phys. Rev. D **69**, 094506 (2004); Phys. Rev. D **73**, 054502 (2006).

[38] G. Akemann, Nucl. Phys. B **730**, 253 (2005); G. Akemann and F. Basile, math-ph/0606060.

[39] G. Akemann, E. Bittner, M. P. Lombardo, H. Markum and R. Pullirsch, Nucl. Phys. Proc. Suppl. **140**, 568 (2005).

[40] G. Akemann and E. Bittner, PoS **LAT2005**, 197 (2006).

[41] P. H. Damgaard, U. M. Heller, K. Splittorff and B. Svetitsky, Phys. Rev. D **72**, 091501 (2005); P. H. Damgaard, U. M. Heller, K. Splittorff, B. Svetitsky and D. Toublan, Phys. Rev. D **73**, 074023 (2006); Phys. Rev. D **73**, 105016 (2006); G. Akemann, P. H. Damgaard, J. C. Osborn and K. Splittorff, hep-th/0609059.

[42] K. Splittorff and J. J. M. Verbaarschot, hep-th/0605143.

[43] J.B. Kogut, M.A. Stephanov, and D. Toublan, Phys. Lett. B **464**, 183 (1999).

[44] J.B. Kogut, M.A. Stephanov, D. Toublan, J.J.M. Verbaarschot, and A. Zhitnitsky, Nucl. Phys. B **582**, 477 (2000).

[45] C. Schmidt, PoS **LAT2006** (2006) 021.

[46] K. Splittorff, hep-lat/0505001.

[47] M. Golterman, Y. Shamir and B. Svetitsky, hep-lat/0602026.